Taimuri, Ghalib; Mikkola, Tommi; Kujala, Pentti; Hirdaris, Spyros

A two-way coupled FSI ship hard grounding dynamics model

Published in:
Proceedings of the 12th International Workshop on Ship and Marine Hydrodynamics

DOI:
10.1088/1757-899X/1288/1/012014

Published: 09/08/2023

Document Version
Publisher's PDF, also known as Version of record

PAPER • **OPEN ACCESS**

A two-way coupled FSI ship hard grounding dynamics model

To cite this article: G Taimuri *et al* 2023 *IOP Conf. Ser.: Mater. Sci. Eng.* **1288** 012014

IOP Conf. Series: Materials Science and Engineering 1288 (2023) 012014 doi:10.1088/1757-899X/1288/1/012014

A two-way coupled FSI ship hard grounding dynamics model

G Taimuri[1, ¥], T Mikkola[1], P Kujala[1] and S Hirdaris[1]

[1] Department of Mechanical Engineering, Aalto University, Espoo, Finland
[¥] Corresponding author: ghalib.taimuri@aalto.fi

Abstract. In the maritime sector, ship grounding incidents continue to be a serious problem that may lead to oil spills, capsizing, severe property damage, and even fatalities. Grounding accidents are currently understood utilizing inadequate statistical datasets, probabilistic grounding scenarios, and deterministic computational crashworthiness methodologies due to a lack of practical tools and techniques. The implementation of multiphysics assessment techniques is essential for the development of improved ship safety standards. This involves the use of rapid models for structural integrity rules and damage stability regulations. Taimuri et al., (2022) [1] introduced a rapid two-way coupled fluid-structure interaction (FSI) model that seeks to efficiently examine accidental loads following a ship hard grounding event to fulfil such a requirement. The current study offers an overview of the algorithm and its limitations.

1. Introduction

To meet safe and sustainable shipping targets, it is essential to proactively reduce the cost of accidents to human life, assets, and the marine environment. Today, despite improvements in technology and crew standards, operational accidents still account for most ship accidents. According to Allianz Global Corporate & Specialty (AGCS) [2] collisions, fires, and groundings are the main causes of catastrophic marine accidents. Navigational accidents caused by collisions, contacts, and groundings continue to dominate ship fatality statistics, making up 43% of all ship-related occurrences between 2014 and 2020, according to European Maritime Safety Agency (EMSA) [3], Figure 1.

The accidental distribution of international marine casualty incidents for various ship types during the period of 2002-2022 has recently been reviewed by Zhang et al. 2023 [4]. According to these findings, the top 5 ship accident records are dominated by container ships, passenger ships, dry cargo vessels (e.g., bulk carriers), tankers, and fishing vessels, Figure 2. Technical problems, routing errors, transportation complications, power failure, loss of ship command, and weather situations are all causes that contribute to ship grounding accidents. In recent years we witnessed a crucial need for increased knowledge of vessel responses following grounding events, especially due to the life cost, the environmental contamination and the expense of these catastrophic events. The Exxon Valdez [5] and Wakashio [6] disasters are examples of ship grounding that polluted the ecosystem. Ship and life loss relate with the accident cases of Express Samina [7], Sea Diamond [8], and Costa Concordia [9]. Recently, the Ever Given accident at the Suez Canal [10], demonstrated that grounding accidents can potentially interrupt marine activities.

To date finite element analysis methods, empirical, experimental, and analytical approaches have been used in consequence modelling. These techniques, however, do not idealise ship maneuverability and the influence of surrounding water on ship dynamics [11]. Ship grounding dynamics are influenced by actions associated with both internal and external mechanics. The former may be used to describe the ship's 6-DoF rigid body motions in response to external inputs and the surrounding water. In hard grounding accidents energy is dissipated when the hull bottom encounters a hard rock leading to structural deformation. Thus, internal mechanics can be used to idealise structural response that results in energy dissipation following contact with the rock.

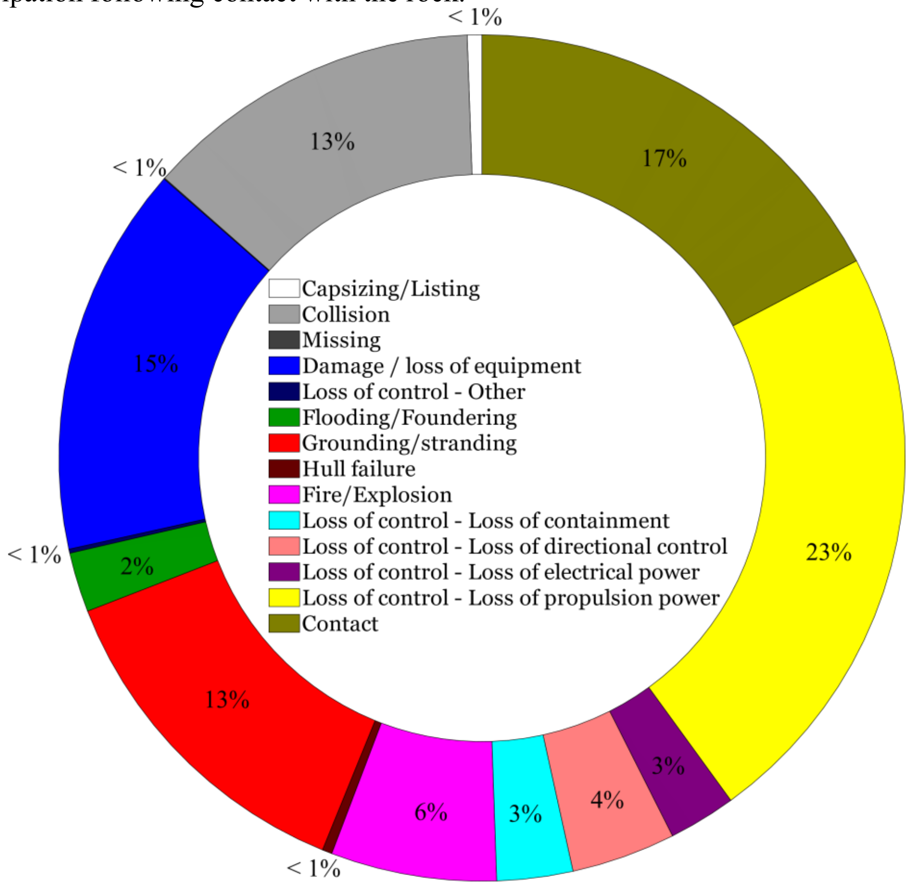

Figure 1. Proportion of incidents involving maritime casualties from 2014 to 2020 [3]

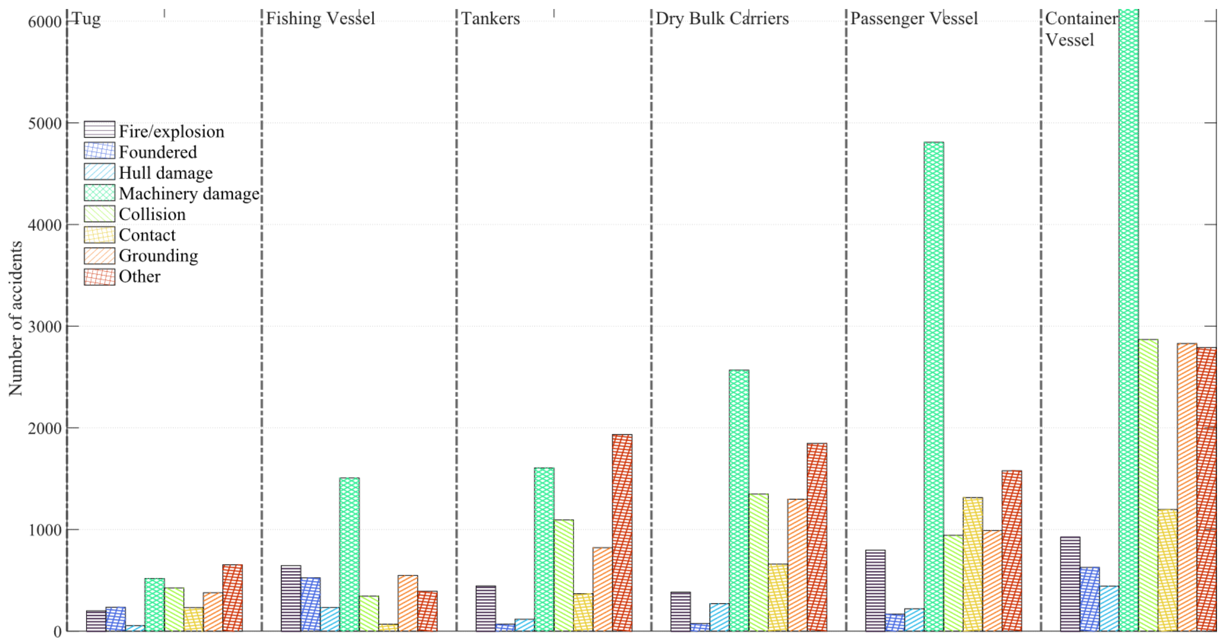

Figure 2. Distribution of global maritime casualty events for different ship types over 2002-2022. [4]

Figure 3 illustrates a review of ship grounding evaluation techniques. The methodologies used to estimate the likelihood of accidents using traffic distributions, historical records, and related risks make up the probabilistic risk evaluation [12]. Using probabilistic statistics to create future predictions may be challenging [13].

Analytical approaches are often employed to assess the crashworthiness of ship structures. The upper-bound theorem is used in these approaches to quantify how much energy is dissipated by major structural components based on the penetration of a rigid object (such as a rock) into a ship's hull. These methods can predict deformations. To analyse internal mechanics analytical formulae are available [14–20]. Yet, the most extensively used and dependable structural response assessment approach is the Finite Element Method (FEM). Despite time consuming FEM is still used in the majority of crashworthiness simulations [20]. Experiments on a big and small scale have been conducted to date [21–27], which are prohibitively expensive, labour-intensive, and may provide findings that are difficult to explain on a full-scale vessel groundings.

Traditionally, external mechanics may be addressed by decoupled methods, which ignore the impact of ship motions on structural deformation. Since these techniques do not adequately capture the consequences of the dynamic impact on a hull surrounded by a fluid, coupled approaches are necessary [28].

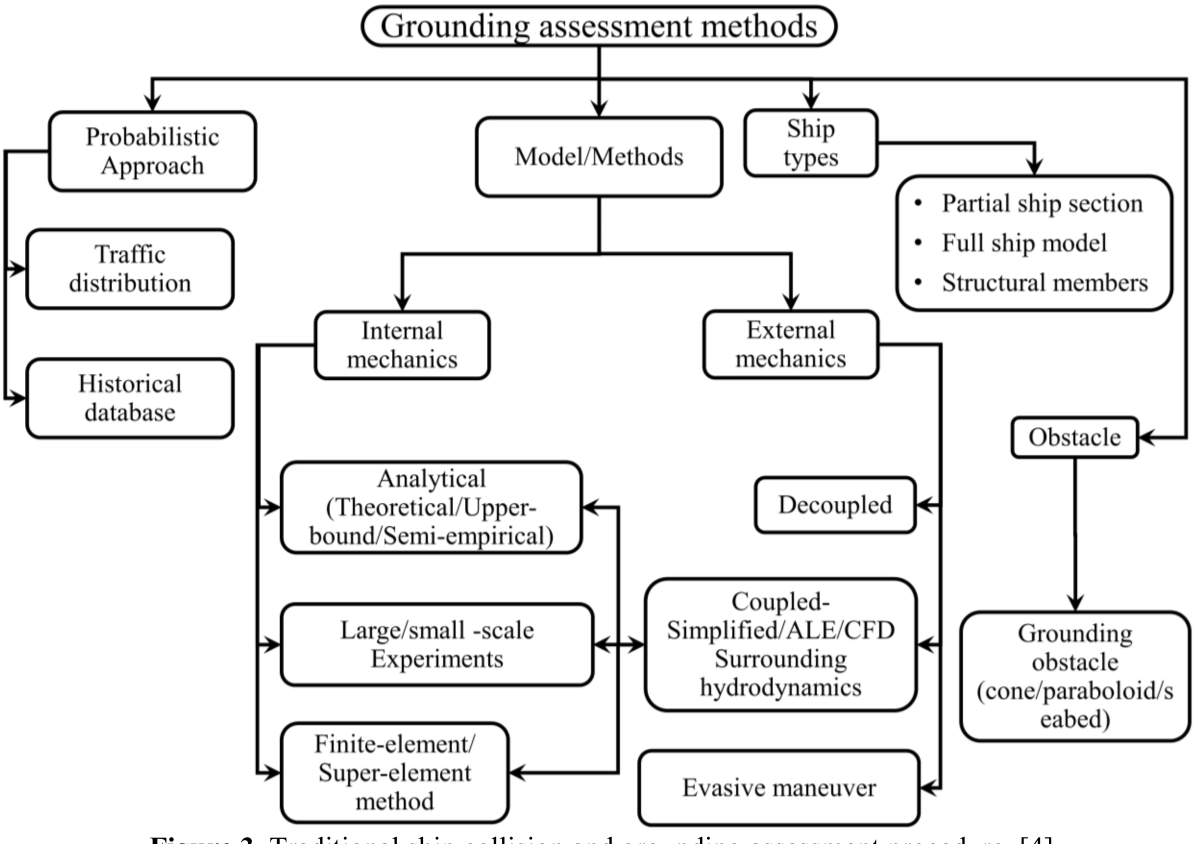

Figure 3. Traditional ship collision and grounding assessment procedure. [4]

The key features and limitations of ship grounding assessment models that have been published during the period of 1997-2022 are depicted in Figure 4. The evaluation is based on internal and external mechanics, investigated vessel types, structural model features, rock forms, and their evaluation. The review demonstrates how little attention has been paid to rapid multiphysics models that idealize coupled ship grounding dynamics [1].

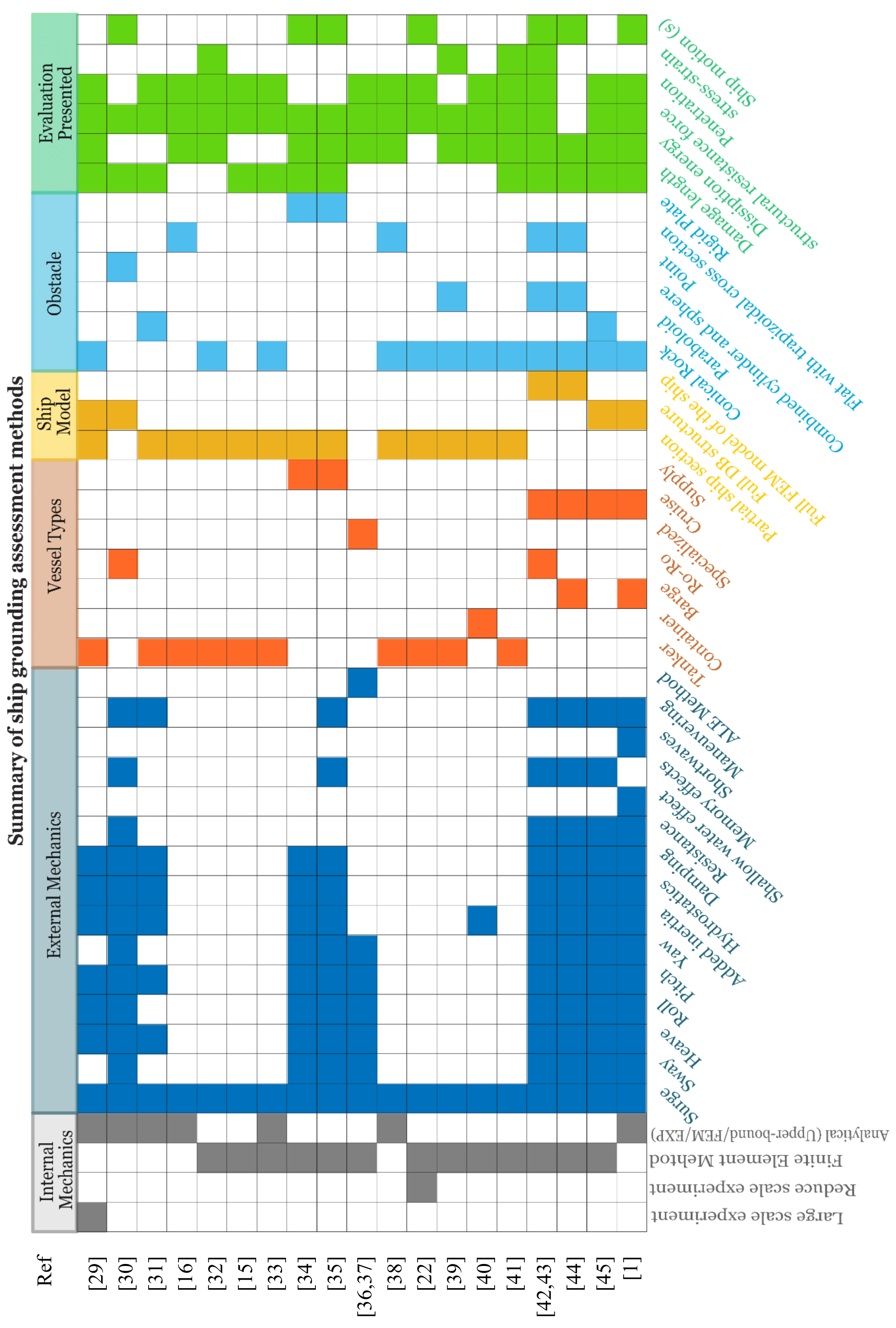

Figure 4. Ship hard grounding assessment methods.

IOP Conf. Series: Materials Science and Engineering 1288 (2023) 012014 doi:10.1088/1757-899X/1288/1/012014

2. Two-way coupled approach

Figure 5 depicts the methods utilized to couple internal and external mechanics. The external mechanics accounts also for possible maneuvering actions. The modelling of a ship's 6-DoF motion during grounding begins with the specification of essential inputssuch as panel mesh of the ship hull, hull hydrodynamic coefficients, rudder-propeller details, and environmental variables. A reference approach for evaluating hydrodynamic hull coefficients is devised for twin screw vessels. For the structural model the rock specification (profile and locations) and ship structural components such as girders, floors, plates, stiffeners, and bulkheads are used. The ship's motions are solved using a set of 2nd-order differential equations, with the ship modelled as a rigid structure navigating in realistic conditions. The contact detection algorithm searches for the interface between the ship panel and the idealized rock After identifying the contact, the structure deforms using an energy approach known as the "upper-bound theorem of plasticity" [40],[46]. The method implies that deformations are influenced by ship motions. Seakeeping actions are considered until the simulation is over, assuming that there is no contact between the rock and hull. Otherwise, the structural deformations caused by the rock and ship bottom contact are incorporated in the ship's 6-DoF motions at each time step. This considers the influences of the sea environment.

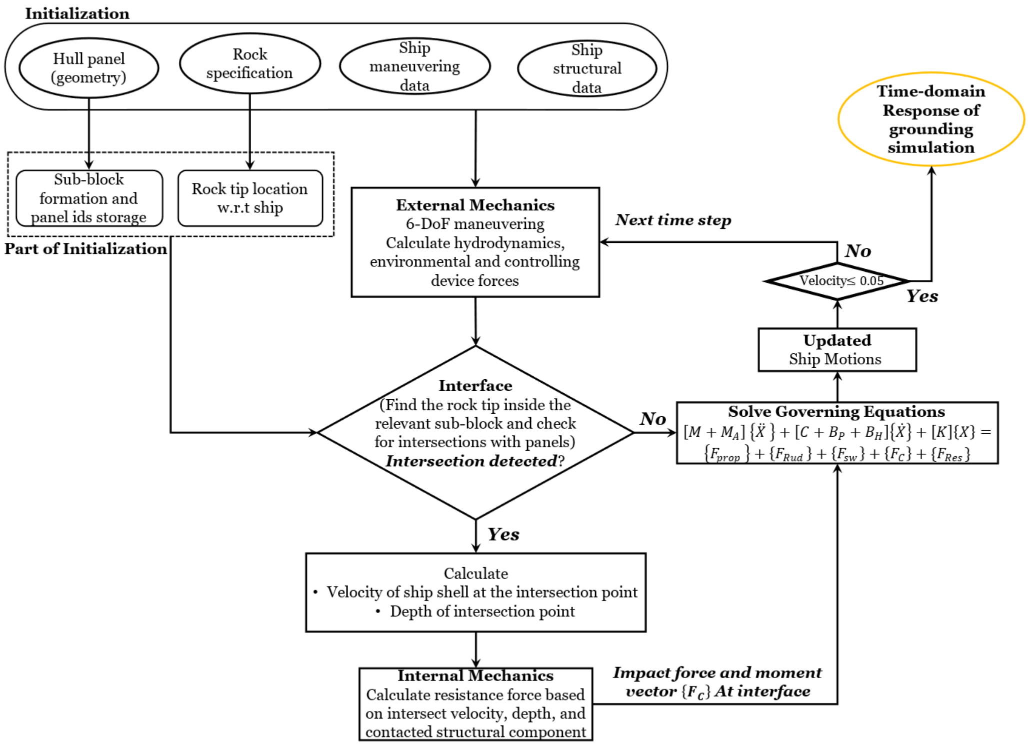

Figure 5. Two-way coupled approach of ship grounding assessment.

3. *Model for coupling ship grounding*

Figure 6 illustrates the coordinate systems utilized for the idealization of a hard grounding event over a rounded-tip conical rock. Using the Earth-fixed coordinate system $O-XYZ$, the vessel's trajectory is determined. The ship's body-fixed origin is measured with reference to the Earth-fixed coordinate system at a distance namely, $\vec{r}=[X_0, Y_0, Z_0]$. The origin of the body-fixed system $(o-xyz)$ is located amidships on an xz-plane of symmetry and at a draft level, where the x-axis points towards the bow, the y-axis towards the starboard side, and the z-axis points downwards. A position vector $\vec{r}_G=[x_G, y_G, z_G]$ is used to define the difference between the center of gravity and the body-fixed origin. Hereby x_G is considered positive towards the bow and z_G is positive towards the base of the ship. The rock location $\vec{r}_{Gr}=[x_{Gr}, y_{Gr}, z_{Gr}]$ is defined as a point node in Earth-fixed coordinate system.

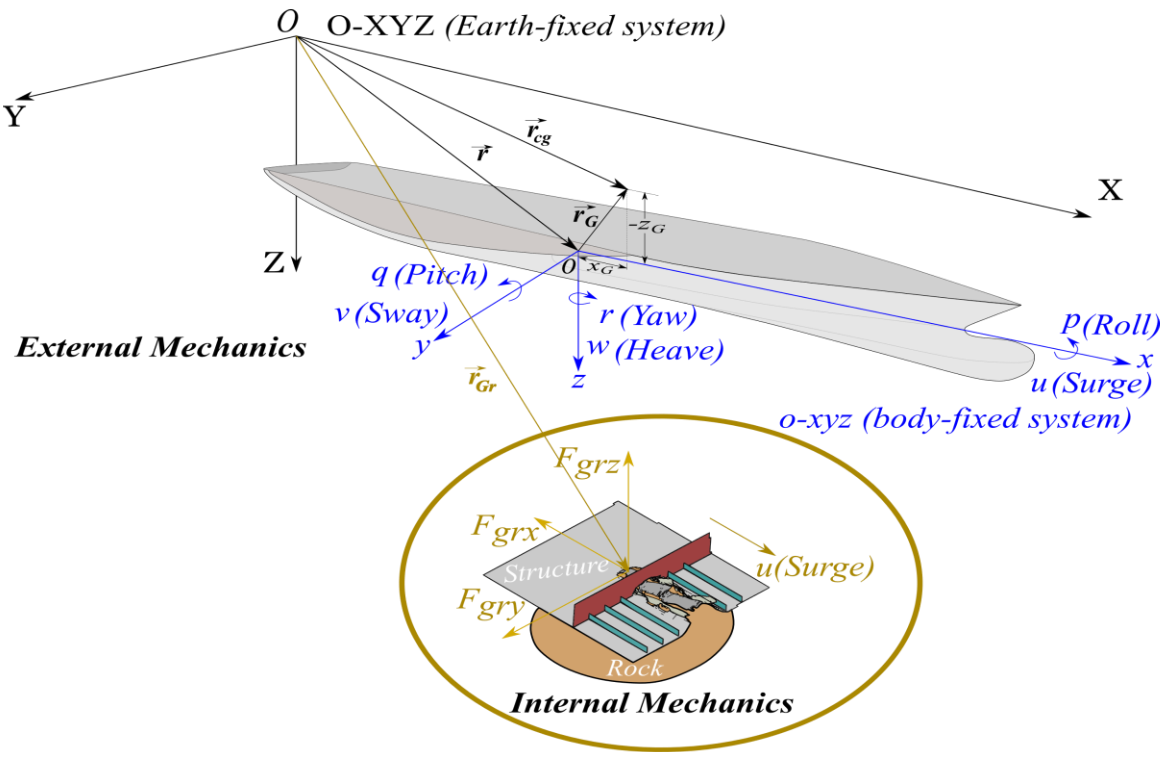

Figure 6. Ship grounding dynamics coordinate system

Assuming a body-fixed system, Figure 6 shows the translational velocity components surge u, sway v, and heave w as well as the rotational velocity components of roll p, pitch q, and yaw r. The fundamental equations describing the mechanics of ship grounding are expressed in Equation (1).

$$
\begin{aligned}
&\text{Surge} && (m - X_{\dot{u}})\dot{u} + (mz_G - 0.5X_{\dot{u}}T) \\
& && \quad = m(rv + x_G(r^2 + q^2) - wq - z_G pr) + \rho g A_{\wp}(\Delta z)sin(\theta) + X_{Hull} \\
& && \quad + X_{Res}(1 - t) + X \quad + X_{Rud} + X_{SW} + X_{C,GRD} \\
&\text{Sway} && (m - Y_{\dot{v}})\dot{v} - \left(mz_G + Y_{\dot{p}}\right)\dot{p} + (mx_G - Y_{\dot{r}})\dot{r} \\
& && \quad = m(\quad - ru - z_G qr - x_G pq) - \rho g A_{\wp}(\Delta z)sin(\phi)cos(\theta) + Y_{Hull} \\
& && \quad + Y_{Rud} + Y_{SW} + Y_{C,GRD} \\
&\text{Heave} && (m - Z_{\dot{w}})\dot{w} - \left(mx_G + Z_{\dot{q}}\right)\dot{q} \\
& && \quad = m(uq - vp + z_G(p^2 + q^2) - x_G rp) - \rho g A_{\wp}(\Delta z)cos(\phi)cos(\theta) \\
& && \quad + \rho g A_{\wp} x_f \theta - 2\zeta_w \omega_w w(m - Z_{\dot{w}}) + Z_{C,GRD} \\
&\text{Roll} && -(mz_G + K_{\dot{v}})\dot{v} + \left(I_X - K_{\dot{p}}\right)\dot{p} - (mx_G z_G + K_{\dot{r}})\dot{r} \\
& && \quad = m(z_G ur - z_G \wp + x_G z_G pq) + (I_Y - I_Z)qr \\
& && \quad - \rho g \nabla GM_T sin(\phi)cos(\phi)cos(\theta) + K_{Hull} + Z_R Y_{Rud} + K_{SW} \\
& && \quad - 2\zeta_\phi \omega_\phi p\left(I_X - K_{\dot{p}}\right) + K_{C,GRD} \\
&\text{Pitch} && (mz_G - 0.5X_{\dot{u}}T)\dot{u} - \left(mx_G + Z_{\dot{q}}\right)\dot{w} + \left(I_Y - M_{\dot{q}}\right)\dot{q} \\
& && \quad = m\left(z_G vr - z_G \left| \quad \right| wq + x_G vp - x_G uq - x_G z_g(p^2 - r^2)\right) \\
& && \quad + (I_Z - I_X)pr - \rho g \nabla GM_L sin(\theta)cos(\phi)cos(\theta) + \rho g A_{\wp} x_f(\Delta z) \\
& && \quad + Z_R X_{Rud} - 2\zeta_\theta \omega_\theta q\left(I_Y - M_{\dot{q}}\right) + M_{C,GRD} \\
&\text{Yaw} && (mx_G - N_{\dot{v}})\dot{v} - (mx_G z_G + K_{\dot{r}})\dot{p} + (I_Z - N_{\dot{r}})\dot{r} \\
& && \quad = m(x_G \wp - x_G ur - x_G z_G qr) + (I_X - I_Y)pq \\
& && \quad - \rho g \nabla(-GM_L cos(\theta) + GM_T)sin(\phi)sin(\theta) + N_{Hull} + X_R Y_{Rud} \\
& && \quad + N_{SW} + N_{C,GRD}
\end{aligned}
\tag{1}
$$

The inertia of the ship, including added masses and moments of inertia, appears on the left side of Equation (1). Semi-empirical relationships or strip theory can be used to estimate these. Coriolis and centripetal forces caused by the rotation of the moving body-fixed system about the Earth-fixed coordinate system are the mass multiplier terms on the right-hand side of Equation (1). The quantities that appear as multiples of acceleration of gravity "g" describe the hydrostatic forces acting on a ship.

The damping of a vessel during maneuvering is represented by in-plane (surge X_{Hull}, sway Y_{Hull}, and yaw N_{Hull}) hydrodynamic damping coefficients. This idealization is based on linear and non-linear semi-empirical relationships. The semi-empirical expression is the outcome of a regression analysis of captive model test (CMT) data. The out-of-plane (heave, roll, and pitch) radiation damping is determined by the ship's natural period (ω_w, ω_ϕ, and ω_θ). The critical damping ratios $\zeta_w, \zeta_\phi \wedge \zeta_\theta$ are calculated using a nonlinear time-domain 6-DoF solver and a numerical decay test. The subscripts "*Res*", "*Prop*", "*Rud*", and "*SW*" represent ship resistance, propeller thrust, control forces, and short-waves forces, respectively.

The behavior of the structure when a ship runs aground over a seabed obstacle is analyzed using the closed-form formulation of structural component resistance forces, represented with a subscript "*C,GRD*" in Equation (1). The depth of penetration of the rock into the hull bottom governs these resistance forces. The procedure considers the bottom structural deformation model introduced by Simonsen [40] and Sun et al. [46]. The formulation is based on the so-called upper bound method of the plastic limit theorem presented in Equation (2).

$$F_H U = F_P . U + \int_S p\mu U_{rel} dS \tag{2}$$

where, F_H is the resistance force of the structure in the direction of relative velocity U between the ship and a rock, F_P is the plastic resistance which includes both plasticity and fracture; μ is the Coulomb coefficient of friction and the last term represents the sliding energy dissipation due to normal and frictional forces on the contact surface of the rock and the plate; U_{rel} is the relative velocity between rock and plate [40].

A conical rock with a rounded tip specified by a radius R_R and semi-apex angle ϕ is used to idealise grounding over a rigid object. The structure consists of the hull's inner and outer shells, longitudinal girders and stiffeners, as well as transverse floors. The forces generated by the deformation of different structural elements are summed together to produce the resultant contact force, which is applied as external forces at the location of the contact, this is represented as a subscript "C,GRD" in Equation (1). Figure 7 depicts the rock profile, structural model, and plate splitting angle after grounding. As the bottom of the hull encounters a rock, the plate tears in a fashion that forms a splitting angle as shown in Figure 7. The magnitude of the plate deformation in front of the conical rock is indicated by this angle. As the energy associated with structural deformation depends on a precise calculation of this angle, it is essential to make a correct assumption in defining the splitting angle. In the previous studies [40,44,46,47], the plate tearing angle was assumed constant throughout the grounding simulation and was precomputed in such a way that it gave the least overall structural resistance force. In other words, the split angle that offers the least amount of resistance is chosen after total structural resistance forces are computed over a range of plate split angles from 0 degrees to 90 degrees. However, this is not the case when a FEM simulation was run, and it was figured out that plate splitting angle depends on the amount of the rock penetrated into the hull, ship motions and the profile of the rock [1]. Taimuri et al. [1], proposed a unique technique to estimate plate splitting angle by utilizing FEM simulation and a curve fitting methodology to develop a plate splitting angle as a function of rock profile and penetration of the rock into the hull. Due to the dynamic nature of the grounding model [1], changes in ship motion will also have an impact on the plate splitting angle.

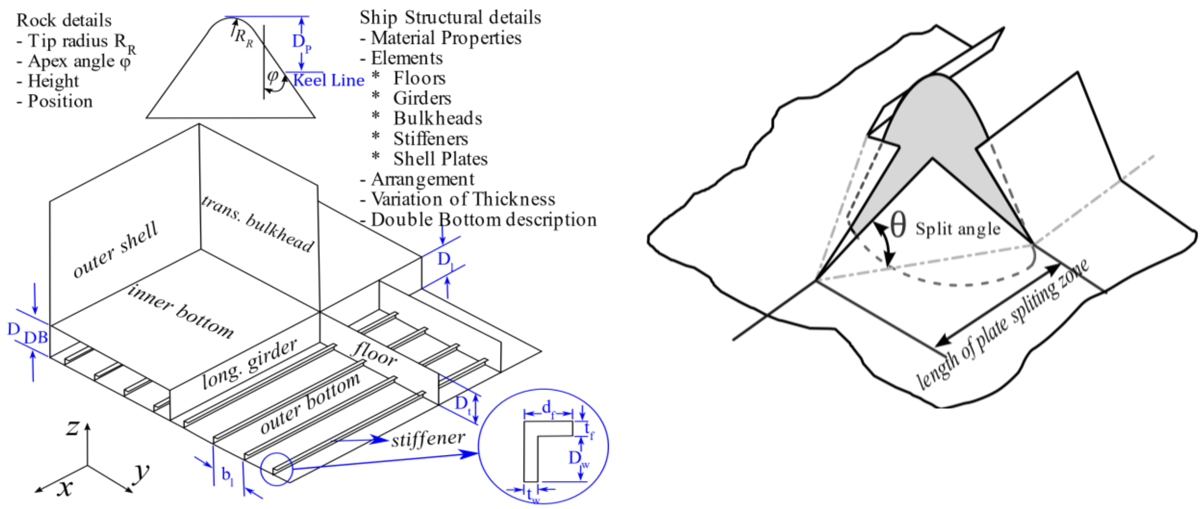

Figure 7. Idealization of ship bottom structure, conical rock, and plate failure mode.

4. Coupling of internal and external mechanics

An ideal vertical line from the rock's tip to the seabed is used to evaluate the contact between the rock's tip and the hull. This results in the displacement of the rock-tip inside the hull namely, δ_{out}. This displacement allows for the calculation of the contact force at the interface, using analytical equations of structural resistance force.

Triangular panels are used to idealise the hull model. Each panel's coordinates are defined in relation to the ship's origin. These panels are saved in the user-defined sub-blocks. The 6-DoF time-domain maneuvering model [1] evaluates the relative location of the hull and the position of the rock tip at each time step. The search for the contact of the rock and the panel starts when the rock tip enters a sub-block. Figure 8 depicts the implementation phases, summed up as follows:

a) Based on the ship's main dimensions, a cartesian grid that surrounds the ship is created. The grid is made up of identical 3D sub-blocks along the length, beam, and depth of the ship.
b) In each 3D sub-bock panels are stored depending on the location of the panels with respect to the 3D sub-block position. The initialization steps under(a) and (b) occur only once.
c) To search for the rock inside the sub-block, the rock tip $\vec{r}_{Gr}$ is changed from an inertial coordinate system to a ship-fixed coordinate system.
d) The vector $\vec{r}_{Gr}$ (Figure 6) is used to identify whether the rock is in the bounding cartesian grid of the ship. If the rock tip is within the cartesian grid, a 3D sub-block containing the rock tip is detected Figure 8. If not, the rock has no effect on the ship structure and the ship will perform her intended movement.
e) A vertical vector is formed, which points towards the base of the seabed from the tip of the rock. If the rock tip is within the 3D sub-block then, this vector is used to search the panel. If a 3D sub-block does not contain panels, then neighbouring block in the direction of vector towards seabed is searched to locate panels. This will follow until the vector reached the edge of the last sub-block in the direction of the vector. If an intersection is found in between above steps the intersection point is stored and the penetration is calculated using a Ray-tracing method [48].
f) The contact coupling model outputs the penetration into the hull following the identification of an intersection. After that, the internal mechanics model receives this penetration and uses it to determine the structural resistance force.

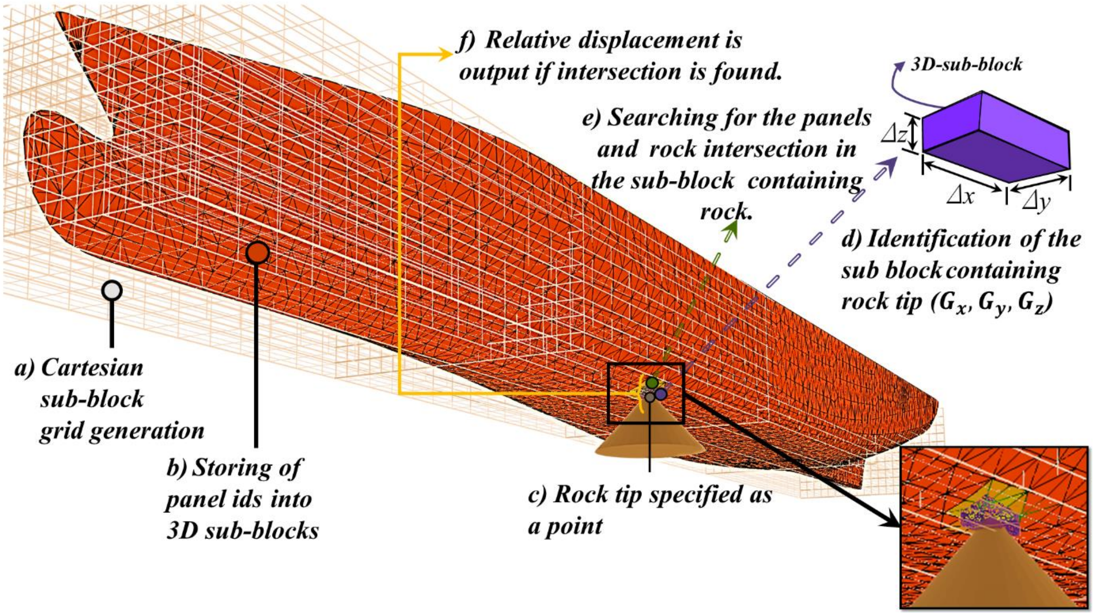

Figure 8. Coupling algorithm details

5. Limitations

The detailed modelling and validation results of the 6-DoF maneuvering model under the influence of the surrounding environment and the comparison coupling algorithm with commercial software LSDYNA can be found in [49] and [1], respectively. The limitation of the models is summarized as follows:

- The hydrodynamic coefficients were evaluated and found to yield satisfactory results for four distinct vessel types. Two different twin-screw and twin-rudder vessels have been validated using the reference approach.
- Drifting of a vessel is considered in shortwaves. As a result, the effect of the waves on heave, pitch, and roll motions is not taken into consideration.
- Yaw-roll hydrodynamic coupling is not taken into consideration. Such modelling could be necessary for a turn at a high speed.
- Pitch motions caused by ship roll are not taken into account. This might result in an underestimation of pitch oscillations during maneuvers. However, the validation of ship off-centre grounding against LS-DYNA MCOL simulations yields satisfactory pitch motions, but the roll motion was overpredicted. These uncertainties need further investigation from the perspective of hydrostatics, and lateral deformation forces of longitudinal members.
- In-plane (hydrodynamic coefficients) and out-of-plane (linear radiation) damping formulations based on regression inherit the memory effects. Yet, memory effects are not specifically considered.
- The plate deformation follows a single clean curling cut. The concertina tearing (plate folding back and forth) and braided cuts (flaps folding back and forth) are not considered. Furthermore, grounding over a conical rock may result in two stable cuts, which is not considered.
- The model overestimates the vertical force in a refined geometric region such as bulbous bow and bilge curves. The model is ideally suited for flat plate interactions.
- The impact of lateral forces on longitudinal girders secured between rocks is not considered.
- The very first contact does not occur between the slant height of the cone and the ship. Instead, the initial contact occurs with the tip of the rock (some distance above the keel base).
- The developed model idealises a rounded tip conical rock. Other shapes are ignored.
- The effect of flooding during an event of grounding and post-grounding is not considered.

6. Conclusions and future study

The goal of developing a two-way coupled rapid FSI grounding dynamics model was to propose a novel and efficient method of assessing ship accidents from a multiphysics viewpoint, as existing numerical methods are time-consuming and large-scale experimentation is impractical. The research establishes the foundation for a computationally efficient technique for coupling external mechanics with internal mechanics. In comparison to LS-DYNA MCOL simulations, which required 4 days of supercomputer time for the simulation, the current FSI model calculation time was reported as being less than 1 second for the same simulation [50]. It is established after successful validation that:

- It is possible to predict the manoeuvring trajectories of both new and existing vessels using the reference technique. The same method can be used to estimate the hydrodynamic activities that will occur in the event of a grounding contact.
- Based on comparisons against experimental data, shallow water and short waves assumptions may be considered acceptable. The same holds for damaged length, breadth, hull penetration, and total deformation energy predicted.
- The assumption of a constant plate split angle approach should be discarded, and structural resistance forces should be evaluated using motion-dependent plate split angles.
- The assumption of linear out-of-plane motions (heave, roll, and pitch) is appropriate for examining grounding dynamics.
- To accurately forecast structural deformation and ship motions, ship restoring forces, damping, and 6-DoF rigid body dynamics must be included. Resistance and shallow water effects have minimal effect on structural resistance force and ship dam-age extents.

Future work should consider hydrodynamic coefficients and their combinations for various hull forms. The lateral loading of the longitudinal elements (girders and stiffeners) is not properly modelled, which results in an underestimation of the lateral forces in an assumed straight-course operation. The severe curvature of the hull's extremities (e.g., bulbous bow region) causes an overestimation of vertical forces. Thus, the model primarily addressed the impact of conical rock profiles and further development of structural resistance force for different rock type are required.

References

[1] Taimuri G, Kim S J, Mikkola T and Hirdaris S 2022 A two-way coupled FSI model for the rapid evaluation of accidental loads following ship hard grounding *J. Fluids Struct.* **112** 103589
[2] Allianz Global Corporate & Specialty 2022 *Safety and Shipping Review 2022 The safety and shipping review from Allianz Global Corporate & Specialty (AGCS) is an annual review of trends and developments in shipping losses, risk challenges and safety*
[3] European Maritime Safety Agency 2021 *Annual overview of marine casualties and incidents - EMSA - European Maritime Safety Agency*
[4] Zhang M, Taimuri G, Zhang J, Zhang D, Yan X and Hirdaris S Ship collision and grounding assessment: State of the art and future perspectives (under review) *Engineering*
[5] Peterson C H, Rice S D, Short J W, Esler D, Bodkin J L, Ballachey B E and Irons D B 2003 Long-term ecosystem response to the Exxon Valdez oil spill *Science (80-.).* **302** 2082–6
[6] Seveso D, Louis Y D, Montano S, Galli P and Saliu F 2021 The Mauritius oil spill: what's next? *Pollutants* **1** 18–28
[7] Papanikolaou A, Spanos D, Boulougouris E, Eliopoulou E and Alissafaki A 2004 Investigation into the sinking of the RO-RO passenger ferry Express Samina *Int. Shipbuild. Prog.* **51** 95–120
[8] Dimitrakakis E, Hahladakis J and Gidarakos E 2014 The "Sea Diamond" shipwreck: Environmental impact assessment in the water column and sediments of the wreck area *Int. J. Environ. Sci. Technol.* **11** 1421–32
[9] Schröder-Hinrichs J U, Hollnagel E and Baldauf M 2012 From Titanic to Costa Concordia—a century of lessons not learned *WMU J. Marit. Aff.* **11** 151–67
[10] Stickings T, Griffith K, Mitchell C, Wright J and Patel B 2021 MailOnline (Suez Canal mega-

ship is on the move) *dailymail*
[11] Bakdi A, Glad I K, Vanem E and Engelhardtsen Ø 2020 AIS-based multiple vessel collision and grounding risk identification based on adaptive safety domain *J. Mar. Sci. Eng.* **8(1)** 1–19
[12] Mazaheri A, Montewka J and Kujala P 2014 Modeling the risk of ship grounding—a literature review from a risk management perspective *WMU J. Marit. Aff.* **13** 269–97
[13] Zhang S, Pedersen P T and Villavicencio R 2019 Probability of ship collision and grounding *Probability and mechanics of ship collision and grounding* ed Butterworth-Heinemann (Kidlington: Matthew Deans) pp 1–61
[14] Haris S and Amdahl J 2013 Analysis of ship–ship collision damage accounting for bow and side deformation interaction *Mar. Struct.* **32** 18–48
[15] Heinvee M and Tabri K 2015 A simplified method to predict grounding damage of double bottom tankers *Mar. Struct.* **43** 22–43
[16] Hong L and Amdahl J 2012 Rapid assessment of ship grounding over large contact surfaces *Ships Offshore Struct.* **7** 5–19
[17] Hong L and Amdahl J 2008 Crushing resistance of web girders in ship collision and grounding *Mar. Struct.* **21** 374–401
[18] Cerup-Simonsen B, Törnqvist R and Lützen M 2009 A simplified grounding damage prediction method and its application in modern damage stability requirements *Mar. Struct.* **22** 62–83
[19] Song M, Kim E, Amdahl J, Ma J and Huang Y 2016 A comparative analysis of the fluid-structure interaction method and the constant added mass method for ice-structure collisions *Mar. Struct.* **49** 58–75
[20] Zhang S, Pedersen P T and Villavicencio R 2019 Internal mechanics of ship collision and grounding *Probability and mechanics of ship collision and grounding* pp 147–270
[21] Calle M A G, Salmi M, Mazzariol L M and Kujala P 2020 Miniature reproduction of raking tests on marine structure: Similarity technique and experiment *Eng. Struct.* **212** 110527
[22] Calle M A G, Oshiro R E and Alves M 2017 Ship collision and grounding: Scaled experiments and numerical analysis *Int. J. Impact Eng.* **103** 195–210
[23] Kitamura O and Kuriowa T 1996 Large-scale grounding experiments and numerical simulations *Sh. Technol. Res.* **43** 62–9
[24] Lemmen P M, Vredeveldt W and Pinkster J A 1996 Design analysis for grounding experiments *International Conference on Designs and Grounding Protection of Ships, San Francisco, California, August 22-23* p 6
[25] Rodd J L and Sikora J P 1995 Double hull grounding experiments *Proceedings of the International Offshore and Polar Engineering Conference* pp 446–56
[26] Rodd J L 1996 Large scale tanker grounding experiments *Proceedings of the International Offshore and Polar Engineering Conference* vol 4 pp 483–94
[27] Tabri K, Määttänen J and Ranta J 2008 Model-scale experiments of symmetric ship collisions *J. Mar. Sci. Technol.* **13** 71–84
[28] Ehlers S 2011 A review of collision and grounding damage assessment methods *Mar. Syst. Ocean Technol.* **6** 5–15
[29] Yu Z, Shen Y, Amdahl J and Greco M 2016 Implementation of linear potential-flow theory in the 6DOF coupled simulation of ship collision and grounding accidents *J. Sh. Res.* **60** 119–44
[30] Lee S G, Zhao T and Nam J H 2013 Structural safety assessment of ship collision and grounding using FSI analysis technique *Collision and Grounding of Ships and Offshore Structures - Proceedings of the 6th International Conference on Collision and Grounding of Ships and Offshore Structures, ICCGS 2013* (Taylor and Francis - Balkema) pp 197–204
[31] Lee S G, Lee J S, Lee H S, Park J H and Jung T Y 2017 Full-scale ship collision, grounding and sinking simulation using highly advanced M&S system of FSI analysis technique *Procedia Engineering* vol 173 (Elsevier Ltd) pp 1507–14
[32] Song Z and Hu Z 2017 An integrated analytical tool on predicting structural responses of ships under collision and grounding scenarios *Proceedings of the International Conference on*

Offshore Mechanics and Arctic Engineering - OMAE, 57656

[33] Prabowo A R, Cao B, Sohn J M and Bae D M 2020 Crashworthiness assessment of thin-walled double bottom tanker: Influences of seabed to structural damage and damage-energy formulae for grounding damage calculations *J. Ocean Eng. Sci.* **5** 387–400

[34] Liu B, Villavicencio R, Pedersen P T and Guedes Soares C 2021 Analysis of structural crashworthiness of double-hull ships in collision and grounding *Mar. Struct.* **76** 102898

[35] Brubak L, Hu Z, Kõrgesaar M, Schipperen I and Tabri K 2021 Numerical simulations of grounding scenarios – benchmark study on key parameters in FEM moddling *Lecture Notes in Civil Engineering* pp 257–69

[36] Kim S J, Kõrgersaar M, Ahmadi N, Taimuri G, Kujala P and Hirdaris S 2021 The influence of fluid structure interaction modelling on the dynamic response of ships subject to collision and grounding *Mar. Struct.* **75** 102875

[37] Kim S J, Kõrgersaar M, Taimuri G, Kujala P and Hirdaris S 2020 A quasi-dynamic approach for the evaluation of structural response in ship collisions and groundings *Proceedings of the International Offshore and Polar Engineering Conference* vol 2020-Octob (International Society of Offshore and Polar Engineers) pp 3174–80

[38] Kim S J, Sohn J M, Kujala P and Hirdaris S 2022 A simplified fluid structure interaction model for the assessment of ship hard grounding *J. Mar. Sci. Technol.* **27** 695–711

[39] Kim S J, Taimuri G, Kujala P, Conti F, Le Sourne H, Pineau J P, Looten T, Bae H, Mujeeb-Ahmed M P, Vassalos D, Kaydihan L and Hirdaris S 2022 Comparison of numerical approaches for structural response analysis of passenger ships in collisions and groundings *Mar. Struct.* **81** 103125

[40] Simonsen B C 1997 *Mechanics of ship grounding. Department of Naval Architecture and Offshore Engineering* (Technical University of Denmark (DTU))

[41] Matusiak J and Varsta P 2002 Transient motion of ship during hard grounding *Proceedings of the 6th International Ship Stability Workshop, Webb Institute, Proceedings. Paper: P2002-1 Proceedings.*

[42] Nguyen T H, Amdahl J, Garrè L and Leira B J 2011 A study on dynamic grounding of ships *Advances in Marine Structures - Proceedings of the 3rd International Conference on Marine Structures, MARSTRUCT 2011* pp 373–80

[43] Abubakar A and Dow R S 2013 Simulation of ship grounding damage using the finite element method *Int. J. Solids Struct.* **50** 623–36

[44] Zeng J, Hu Z and Chen G 2016 A steady-state plate tearing model for ship grounding over a cone-shaped rock *Ships Offshore Struct.* **11** 245–57

[45] Yu Z and Amdahl J 2016 Full six degrees of freedom coupled dynamic simulation of ship collision and grounding accidents *Mar. Struct.* **47** 1–22

[46] Sun B, Hu Z and Wang J 2017 Bottom structural response prediction for ship-powered grounding over rock-type seabed obstructions *Mar. Struct.* **54** 127–43

[47] Friis-Hansen P and Simonsen B C 2002 GRACAT: Software for grounding and collision risk analysis *Mar. Struct.* **15**

[48] Moller T and Trumbore B 1997 Fast, minimum storage ray-triangle intersection *J. Graph. Tools* **2** 21–8

[49] Taimuri G, Matusiak J, Mikkola T, Kujala P and Hirdaris S 2020 A 6-DoF maneuvering model for the rapid estimation of hydrodynamic actions in deep and shallow waters *Ocean Eng.* **218** 108103

[50] Taimuri G H 2022 *A fully coupled Fluid Structure Interaction model for assessing ship hard grounding dynamics* (Aalto University)